

## Exit probability in inflow dynamics: Nonuniversality induced by range, asymmetry, and fluctuation

Parna Roy,<sup>1,\*</sup> Soham Biswas,<sup>2</sup> and Parongama Sen<sup>1</sup>

<sup>1</sup>*Department of Physics, University of Calcutta, 92 Acharya Prafulla Chandra Road, Kolkata 700009, India*

<sup>2</sup>*Department of Theoretical Physics, Tata Institute of Fundamental Research, Homi Bhabha Road, Mumbai 400 005, India*

(Received 16 January 2014; published 31 March 2014)

Probing deeper into the existing issues regarding the exit probability (EP) in one-dimensional dynamical models, we consider several models where the states are represented by Ising spins and the information flows inwards. At zero temperature, these systems evolve to either of two absorbing states. The EP,  $E(x)$ , which is the probability that the system ends up with all up spins starting with  $x$  fraction of up spins, is found to have the general form  $E(x) = x^\alpha / [x^\alpha + (1-x)^\alpha]$ . The EP exponent  $\alpha$  strongly depends on  $r$ , the range of interaction, the symmetry of the model, and the induced fluctuation. Even in a nearest-neighbor model, a nonlinear form of the EP can be obtained by controlling the fluctuations, and for the same range, different models give different results for  $\alpha$ . Nonuniversal behavior of the EP is thus clearly established and the results are compared to those of existing studies in models with outflow dynamics to distinguish the two dynamical scenarios.

DOI: [10.1103/PhysRevE.89.030103](https://doi.org/10.1103/PhysRevE.89.030103)

PACS number(s): 64.60.De, 89.75.Da, 89.65.-s

There are many systems in condensed matter physics, magnetism, biology, and social phenomena [1–4] which are found to reach an ordered state following certain dynamical rules. The dynamical rules represent the mechanisms by which macroscopic structures are generated from microscopic interactions. The role of the dynamics is reflected in the scaling behavior of relevant variables. Often we note power law scaling behavior; e.g., in coarsening phenomena, domains grow in a power law manner with time. If two different dynamical schemes lead to identical behavior of the relevant variables, one may conclude that the two schemes are actually equivalent. However, careful studies are required to establish such equivalence.

Of late, a debate on whether inflow dynamics is different from outflow dynamics has emerged [5–8]. Precisely, in models involving spins, when the state of the central spin is dictated by its neighbors, it is a case of inflow of information. Outflow of information occurs when a group of neighboring spins dictates the state of all other spins neighboring them. To settle the debate, the exit probability (EP) is one of the features which is studied when the spins can be in up or down states. Starting with  $x$  fraction of spins in the up state, the EP  $E(x)$  is the probability of reaching a final state with all spins up.

The Ising-Glauber model [5] is an example of inflow dynamics where the local field determines whether or not a spin will flip. An example where outflow of information takes place is the Sznajd model [6]. In the Ising-Glauber model, a spin is selected randomly and its state is updated following an energy minimization scheme. In one dimension, this always leads to either of two absorbing states: all spins up or all down. In the Sznajd model, a plaquette of neighboring spins is considered; if they agree, then the spins on the boundary of the plaquette are oriented along them. In one dimension, the plaquette is a panel of two spins. The Sznajd model has the same two absorbing states as in the Ising model. The two models also have identical exponents associated with domain growth and persistence behavior during coarsening [9,10]. However, a

few other dynamic quantities were shown to be different for generalized models with inflow and outflow dynamics where a suitable parameter associated with the spin-flip probability was introduced [7,11]. The Ising-Glauber and Sznajd models can be obtained by choosing specific values of the parameters in the generalized models with inflow and outflow dynamics, respectively.

The EP plays an important role in the debate, as it shows a marked difference in behavior for the two models: for the Ising-Glauber model the EP is linear,  $E(x) = x$ , while for the Sznajd model [8,12,13]

$$E(x) = \frac{x^2}{x^2 + (1-x)^2}, \quad (1)$$

a distinctly nonlinear function of  $x$ .

Another version of a generalized model with inflow and outflow dynamics was proposed more recently [8] in which the range  $r$  of the interaction was varied. The Sznajd model with range  $r$  [S( $r$ ) model] showed a range-independent behavior of the EP; the EP is given by Eq. (1) for all  $r$ . For the generalized Ising-Glauber model with  $r$  neighbors [G( $r$ ) model], numerical simulations were made which showed a very good fit to the form given in Eq. (1) for  $r = 2$ , from which it was claimed that nonlinear behavior of  $E(x)$  can be observed for inflow dynamics as well.

A generalized  $q$ -voter model which involves outflow dynamics has also been proposed [14], in which  $q$  neighboring spins, if they agree, influence their other neighboring spins. In one dimension,  $q = 2$  corresponds to the Sznajd model, and the random version with  $q = 1$  (where only one of the two boundary spins is updated with equal probability) corresponds to the Ising-Glauber/voter model. The EP here, again, showed the property of being independent of range.

The shape of the EP is an important issue. Another interesting point to be noted is, in all the models studied so far [8,12–14] in one dimension, no finite-size dependence has been noted in the EP. However, there is a school of thought that such effects do exist, and in reality the EP has a step function behavior in the thermodynamic limit [15] as observed in higher dimensions [16–18]. Such step function behavior also

\*parna.roy14@gmail.com

occurs for a special class of one-dimensional models where the dynamical rule involves the size of the neighboring domains [19,20]. However, in the present work, we consider only those models with inflow dynamics (all of which are short range) which belong to the Ising-Glauber class as far as dynamical behavior is concerned. Our aim is to find out how the EP depends on various factors incorporated in the dynamics. Our main result is that a general form for the EP given by

$$E(x) = \frac{x^\alpha}{x^\alpha + (1-x)^\alpha} \quad (2)$$

exists, where  $\alpha$ , the so-called EP exponent, is very much dependent on factors like the range of interaction, asymmetry of the model, and fluctuation present in the dynamics.

Here we summarize the models and results.

(1) The Ising-Glauber model with  $r$  neighbors [G(r)]: To update the  $i$ th spin  $s_i (= \pm 1)$  here, one computes

$$x = \sum_{j=1}^r [s_{i+j} + s_{i-j}]. \quad (3)$$

If  $x > 0$ ,  $s_i = 1$ , if  $x < 0$ ,  $s_i = -1$  and  $s_i$  is flipped with probability  $1/2$  if  $x = 0$ . For G(r), results are known for  $r = 1$  (exact) [3] and 2 (numerical) [8]. We have obtained results for higher values of  $r$ .

(2) The cutoff model: A model with a cutoff at  $r$  called the C(r) model, proposed in [21], was also studied. Here only the spins sitting at the domain boundary are liable to flip. To update such a spin at site  $i$ , we calculate two quantities,  $r_1$  and  $r_2$ .  $r_1$  is determined from the condition

$$s_{i+1} = s_{i+2} = \dots = s_{i+r_1} \neq s_{i+r_1+1}; \quad (4)$$

and similarly,  $r_2$  is calculated from the spins on the left side of the  $i$ th spin.  $r_1$  and  $r_2$  are both restricted to a maximum value  $r$ . Hence the neighboring domain sizes  $r_1$  and  $r_2$  are calculated subject to the restriction that the maximum size is  $r$ . When  $r_1$  is greater (less) than  $r_2$ , the state of the right (left) neighbors is adopted. If  $r_1 = r_2$ , the spin is flipped with probability  $1/2$ . C(r) is equivalent to G(r) for  $r = 1$ .

(3) The ferromagnetic asymmetric (FA) model: The G(2) and C(2) models can in fact be shown to be special cases of the Ising model with second-neighbor interaction. The Hamiltonian for this model is

$$H = -J_1 \sum_i s_i s_{i+1} - J_2 \sum_i s_i s_{i+2}. \quad (5)$$

Here, the role of asymmetry can be studied by varying  $\kappa = J_2/J_1$ . The special case  $\kappa = 1$  is identical to G(2).  $\kappa < 1$  corresponds to C(2), and for  $\kappa > 1$  one may expect a different behavior. This system can be regarded as an ANNNI chain [22] with both interactions positive (ferromagnetic). By definition the FA model has range  $r = 2$ .

(4) The W(r) model: The W(r) model is exactly like the Ising-Glauber model except for the fact that when  $x = 0$  in Eq. (3), the spins are flipped with probability  $W_0$  [11]. It is known that for  $W_0 = 0$ , which is called the constrained Glauber model, absorbing states are frozen states which are not all-up or all-down states.  $W_0 = 0.5$  corresponds to the Ising Glauber model, while  $W_0 = 1$  is the case of the metropolis rule.  $W_0$  in a sense quantifies the fluctuation induced by the

Configurations of the neighboring spins	Updated central spin for the different dynamical rules			
	G(1)	G(2)	C(2)	FA
↓ ↓ ● ↓ ↓	↓	↓	↓	↓
↓ ↓ ● ↓ ↑	↓	↓	↓	↓
↓ ↓ ● ↑ ↓	○	↓	↓	↓
↓ ↓ ● ↑ ↑	○	○	○	○
↓ ↑ ● ↓ ↓	○	↓	↓	↓
↓ ↑ ● ↓ ↑	○	○	○	○
↓ ↑ ● ↑ ↓	↑	○	↑	↑ ( $J_1 > J_2$ )
↓ ↑ ● ↑ ↑	↑	↑	↑	○ ( $J_1 = J_2$ )
↓ ↑ ● ↓ ↓	↑	↑	↑	↓ ( $J_1 < J_2$ )
↓ ↑ ● ↑ ↑	↑	↑	↑	↑

FIG. 1. (Color online) Left: Configuration of the neighboring spins of the central spin, represented by a filled circle, which means either of the up or down states at time  $t$ . Right: State of the central spin after it is updated according to the different dynamical rules. An open circle implies an “undecided” state when the up and down state occur with equal probability. The other eight states can be obtained by inversion.

dynamics; the fluctuation is maximum when  $W_0 = 1$ , which causes the spins to flip whenever  $x$  in Eq. (3) equals 0. In this model, we have studied the case for  $r \geq 1$ .

In Fig. 1, we present the possible updated configurations for the central spin corresponding to eight configurations of its four nearest neighbors for G(1), G(2), C(2), and FA. The other eight cases can be obtained by inverting all the spins. It is immediately noted that G(r) and C(r) differ even for  $r = 2$ . For FA, we may expect a new value of  $\alpha$  for  $\kappa > 1$ , which, however, should not depend on the exact value of the  $\kappa$ . It is also seen that the central spin is “undecided” in the maximum number of cases in G(1); there are fewer such cases for G(2) and even fewer for C(2) and FA with  $\kappa \neq 1$ . We discuss the effect of this feature on the EP later.

As mentioned before, the EP follows a behavior given by Eq. (2) in all cases. Typical variation of the EP for G(r) and C(r) for  $r = 3$  are shown in Fig. 2. In Fig. 3, we plot the values of  $\alpha$  against  $r$  for these two models. We note that  $\alpha$  is an increasing function of  $r$  for both models. Hence  $\alpha$  for G(r) is greater than 2 for  $r > 2$  and the value of  $\alpha = 2$  coincides with the S(r) value only for  $r = 2$ . On the other hand,  $\alpha$  is less for C(r) compared to G(r) for all  $r > 1$ . We try a general form to fit  $\alpha$  with  $r$ ,

$$(\alpha - 1) = a(r - 1)^b, \quad (6)$$

and note that it shows a fairly good fit for both G(r) and C(r), with  $a = 1.04 \pm 0.02$ ,  $b = 0.66 \pm 0.02$  for G(r) and

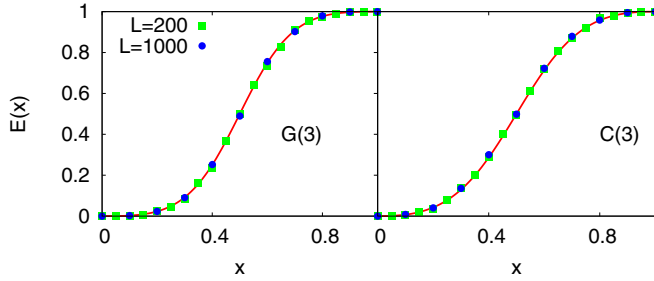


FIG. 2. (Color online) Exit probability versus initial concentration of up spins in the generalized Ising [G( $r$ ); left] and cutoff [C( $r$ ); right] models with  $r = 3$ . The  $L = 1000$  curves are fitted with the best-fit line of the form given in Eq. (2).

$a = 0.85 \pm 0.01$ ,  $b = 0.56 \pm 0.01$  for C( $r$ ). Both  $a$  and  $b$  are larger for G( $r$ ), indicating a stronger dependence on  $r$ .

The FA model, as expected, gives  $\alpha = 1.85 \pm 0.03$  for  $\kappa < 1$ , which is identical to the C(2) value ( $1.85 \pm 0.02$ ) and  $\alpha = 2$  for  $\kappa = 1$  [G(2) model]. In the third case,  $\kappa > 1$ , we get the new value of  $\alpha = 2.24 \pm 0.04$ . The results are shown in Fig. 4.

The W( $r$ ) model leads to both qualitatively and quantitatively different results. Even for  $r = 1$ , the EP does not have a linear dependence on  $x$  for  $W_0 \neq 0.5$ ;  $\alpha \neq 1$ , unlike the Ising-Glauber case (Fig. 5). Here too we find  $\alpha$  to be dependent on  $r$ . We plot the dependence of  $\alpha$  against  $W_0$  for  $r = 1, 2$ , and 3 in Fig. 6. For the W(1) model,  $\alpha$  behaves as  $1/\sqrt{2W_0}$  as  $W_0 \rightarrow 1$ . The values of  $\alpha$  for  $r = 2$  and  $r = 1$  differ by unity for any  $W_0$  as in the Ising-Glauber model. However, the differences in the values of  $\alpha$  for W(3) and W(2) weakly increase with  $W_0$ . It is interesting to note here that the Glauber ( $W_0 = 0.5$ ) and metropolis ( $W_0 = 1$ ) algorithms give different values of  $\alpha$ , although for any  $W_0 \neq 0$ , the W( $r$ ) model belongs to the Glauber universality class [11].

Some general features can immediately be noted from the results. If  $r$  is increased,  $\alpha$  increases, indicating that the EP becomes steeper in models with inflow dynamics. When  $r$  is the same in the two models,  $\alpha$  assumes different values due to the presence of other factors. For example, both G(2) and FA ( $\kappa > 1$ ) have  $r = 2$ , but  $\alpha$  is larger in the latter. The two models differ in the number of so-called “undecided states” (see Fig. 1), and apparently  $\alpha$  is larger when such states are fewer in number. In order to account for the fact that C(2) has

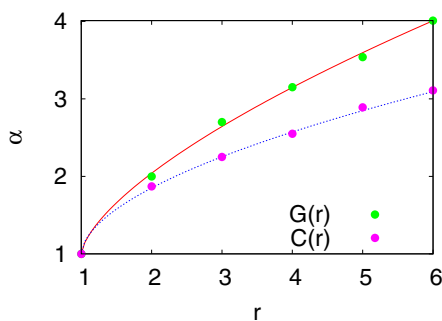


FIG. 3. (Color online) Plot of the exponent  $\alpha$  against the range  $r$  for G( $r$ ) and C( $r$ ) models. The solid line corresponds to the fitting form of Eq. (6).

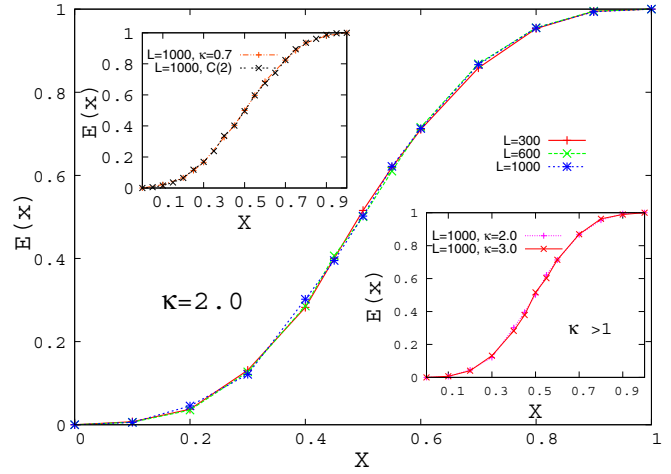


FIG. 4. (Color online) Exit probability for the FA model: plot shows the result for  $\kappa = 2$  for different system sizes. Top-left inset:  $E(x)$  for  $\kappa < 1$  and C(2), which give identical results as expected. Bottom-right inset: For  $\kappa > 1$ , the EP is independent of the exact value of  $\kappa$ . The solid lines are guides for the eye.

a smaller value of  $\alpha$  compared to G(2), although the number of undecided states is lower here, one must also note that the effective number of neighbors in C(2) is less than 2. The combined effect makes the value of  $\alpha$  smaller, indicating that the range has a stronger effect on the EP than the stochasticity.

The results in the W( $r$ ) model can be qualitatively explained. For  $r = 1$ , we note that the EP curves have different curvatures for  $W_0$  below and above 0.5. Let us take the case of  $x < 0.5$ , where the EP is larger for  $W_0 > 0.5$  than for  $W_0 = 0.5$ . This happens since the initial state here contains more spins in the down state, and the flipping probability is higher than  $1/2$ . The same logic explains why the EP is lower when  $x > 0.5$ . At  $x = 0.5$ ,  $E(x)$  is equal to  $1/2$  for all models as  $E(x) + E(1-x) = 1$ . So the curves cross at  $x = 0.5$  and  $\alpha$  has a value of  $< 1$  for  $W_0 > 0.5$  and a value of  $> 1$  for  $W_0 < 0.5$  [as for  $W_0 = 0.5, E(x) = x$ , or  $\alpha = 1$ ].  $W_0$  effectively control the fluctuation and we find that it can alter the value of  $\alpha$ . For larger values of  $r$ , similarly,  $\alpha$  is larger (smaller) than the G( $r$ ) values for  $W_0 < 0.5$  ( $W_0 > 0.5$ ). However, the curvatures are the same as  $\alpha > 1$  always.

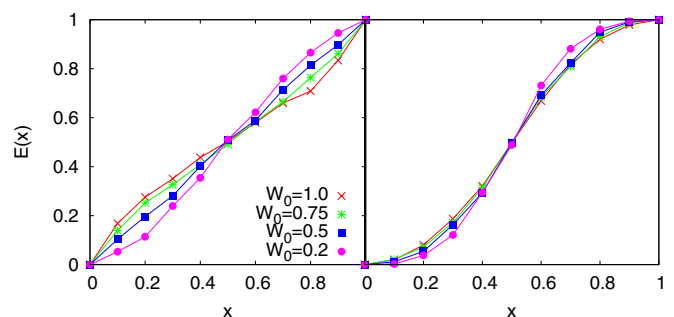


FIG. 5. (Color online) Exit probability versus initial concentration of up spins in the W( $r$ ) model:  $r = 1$  (left) and  $r = 2$  (right). Solid lines are guides for the eye.

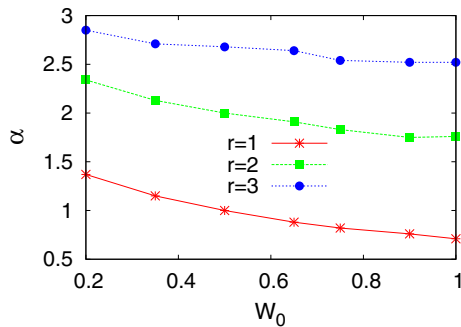


FIG. 6. (Color online) Exponent  $\alpha$  versus  $W_0$  in the  $W(r)$  model with  $r = 1, 2$ , and  $3$ . Solid lines are guides for the eye.

We also note that no system size dependence of the EP is observed in any of the models even when  $r$  is increased, asymmetry is introduced, or fluctuation is modified. So there is no indication of a step function like the EP for finite values of  $r$  even in the thermodynamic limit. However, as  $r$  is made larger,  $\alpha$  increases, and one can conclude that in the fully connected model corresponding to the infinite-dimensional case,  $\alpha$  will diverge, giving rise to a step function behavior in the EP at  $x = 1/2$ .

Some of the issues discussed at the beginning of the paper may be addressed now. First, it is evident that the EP shows range dependence in models with inflow of information in general, in contrast to models with outflow of information, where increasing the range only results in a change in time scales. In inflow dynamics, increasing  $r$  apparently makes the system approach higher dimensional behavior, although no system-size dependence appears. The fact that the EPs for the  $S(r)$  and  $G(2)$  models [8,13,14] show identical behavior ( $\alpha = 2$ ) seems to be purely accidental; there are inflow and outflow models with  $r = 2$  which have  $\alpha \neq 2$ . However,  $\alpha$  can be nonintegral in inflow dynamics, in contrast to known models with outflow dynamics [8,14] ( $\alpha = q$  for the  $q$  voter model).

An important issue is the question of universality. As already mentioned, all the models studied here have the

same dynamical behavior as far as coarsening is concerned; they all belong to the Ising-Glauber class with the dynamic exponent and persistence exponent identical. In fact, even the models with outflow dynamics like the Sznajd model belong to this universality class [10] (we have checked for  $r = 2$  as well). Thus we find that the EP is a nonuniversal quantity; it depends on the details of the dynamical rule and is not simply determined by whether information flows out or in. However, it seems safe to state that there is a clear difference: outflow dynamics is characterized by the absence of range dependence while inflow dynamics shows range dependence.

The question that may naturally arise after this discussion is, Why does the EP behave differently when the coarsening behavior is identical? Here it should be remembered that coarsening behavior is strictly relevant to a completely random initial configuration corresponding to  $x = 1/2$ . Indeed, at  $x = 1/2$ , in all cases  $E(x) = 1/2$ . Hence a deviation from the perfectly random state results in reaching all-up or all-down states with different probabilities for the different models.

In summary, we present evidence that the EP can be expressed in a general form. An exponent  $\alpha$  associated with the EP is identified which is strongly dependent on the details of the system as far as inflow dynamics is concerned.  $\alpha$  can have nonintegral values (even less than unity) for inflow dynamics, while for the models with outflow dynamics studied so far, only integral values have been obtained. Most of the observed results can be qualitatively explained.

The range dependence distinguishes inflow dynamics from outflow dynamics. Apart from the range dependence, other factors in the dynamical rules also affect the EP in inflow dynamics. The effects of these factors on outflow dynamics may reveal further distinguishing features; a study is in progress [23].

S.B. thanks the Department of Theoretical Physics, TIFR, for the use of its computational resources. P.R. acknowledges financial support from UGC. P.S. acknowledges financial support from the CSIR project.

- 
- [1] A. M. Turing, *Phil. Trans. Roy. Soc. B* **237**, 37 (1952).  
 [2] A. J. Bray, *Adv. Phys.* **43**, 357 (1994).  
 [3] P. Sen and B. K. Chakrabarti, *Sociophysics: An Introduction* (Oxford University Press, Oxford, UK, 2013).  
 [4] C. Castellano, S. Fortunato, and V. Loreto, *Rev. Mod. Phys.* **81**, 591 (2009).  
 [5] R. J. Glauber, *J. Math. Phys.* **4**, 294 (1963).  
 [6] K. Sznajd-Weron and J. Sznajd, *Int. J. Mod. Phys. C* **11**, 1157 (2000).  
 [7] K. Sznajd-Weron and S. Krupa, *Phys. Rev. E* **74**, 031109 (2006).  
 [8] C. Castellano and R. Pastor-Satorras, *Phys. Rev. E* **83**, 016113 (2011).  
 [9] L. Behera and F. Schweitzer, *Int. J. Mod. Phys. C* **14**, 1331 (2003).  
 [10] D. Stauffer and P. M. C. de Oliveira, *Eur. Phys. J. B* **30**, 587 (2002).  
 [11] C. Godrèche and J. M. Luck, *J. Phys: Condens. Matter* **17**, S2573 (2005).  
 [12] R. Lambiotte and S. Redner, *Europhys. Lett.* **82**, 18007 (2008).  
 [13] F. Slanina, K. Sznajd-Weron, and P. Przybyla, *Europhys. Lett.* **82**, 18006 (2008).  
 [14] P. Przybyla, K. Sznajd-Weron, and M. Tabiszewski, *Phys. Rev. E* **84**, 031117 (2011).  
 [15] S. Galam and A. C. R. Martins, *Europhys. Lett.* **95**, 48005 (2011), and references therein.  
 [16] D. Stauffer, A. O. Sousa, and S. M. de Oliveira, *Int. J. Mod. Phys. C* **11**, 1239 (2000).  
 [17] N. Crockidakis and P. M. C. de Oliveira, *J. Stat. Mech.* (2011) P11004, and references therein.  
 [18] C. Castellano and R. Pastor-Satorras, *Phys. Rev. E* **86**, 051123 (2012).  
 [19] S. Biswas, S. Sinha, and P. Sen, *Phys. Rev. E* **88**, 022152 (2013).  
 [20] P. Roy, S. Biswas, and P. Sen, *arXiv:1403.2199*.  
 [21] S. Biswas and P. Sen, *J. Phys. A: Math. Theor.* **44**, 145003 (2011).  
 [22] W. Selke, *Phys. Rep.* **170**, 213 (1988).  
 [23] P. Roy and S. Biswas (unpublished).